JOURNAL OF CATALYSIS **177,** 82–95 (1998)
ARTICLE NO. CA982094

# Nature of Copper Active Sites in the Carbon Monoxide Oxidation on $CuAl_2O_4$ and $CuCr_2O_4$ Spinel Type Catalysts

F. Severino,*[,1] J. L. Brito,* J. Laine,* J. L. G. Fierro,† and A. López Agudo†[,2]

*Laboratorio de Fisicoquímica de Superfícies, Centro de Química, Instituto Venezolano de Investigaciones Científicas, I.V.I.C. Apartado 21827, Caracas 1020-A, Venezuela; and †Instituto de Catálisis y Petroleoquímica, Campus UAM, Cantoblanco, 28049 Madrid, Spain

Received October 20, 1997; revised March 24, 1998; accepted March 24, 1998

**Unsupported copper-aluminum and copper-chromium oxides were prepared by mixing solutions of the nitrates and calcining at 1223 K, followed by treatment with washing solutions of either ammonium carbonate or nitric acid in order to extract uncombined copper oxide. Ammonium carbonate was only effective for removal of dispersed CuO, whereas nitric acid removed both dispersed and crystalline CuO. Catalyst activity for CO oxidation increased with the extraction treatments, particularly with the nitric acid washing solution, indicating that the active sites are copper species derived from $CuAl_2O_4$ and $CuCr_2O_4$ spinels rather than from CuO. The $CuCr_2O_4$ catalyst exhibited higher activity, suggesting that Cu species in tetrahedral coordination lead to higher activity. Also, prereduction with $H_2$ produced higher activity than prereduction with CO, which can be attributed to a higher surface concentration of active species or their precursors after the former treatment. Activity results, together with TPR and XPS characterization point out that both $Cu^0$ and $Cu^+$ species are involved in the mechanism of CO oxidation.** 

## INTRODUCTION

Copper-based oxides are catalysts for a variety of important reactions (1–4), including CO oxidation which is related to both fundamental and pollution control studies (5–7). Although noble metal systems work very well for this reaction, the so-called base metal catalysts have deserved increasing attention for their significant activity and lower cost. Among the base metal catalysts, the copper–chromium pair seems to be one of the most efficient (8, 9). Although several studies have been reported on the characterization of alumina-supported copper oxide catalysts (10–13), a clear correlation between activity for CO oxidation and catalyst structure has not been found. In the more interesting copper–chromium-based catalysts the information is even more scarce.

In previous work, attempts have been made to relate surface structure and composition of supported Cu and Cu–Cr oxide catalysts with the catalytic behaviour (13–15), suggesting that the locus of catalytic activity for CO oxidation is a copper center. However, the specific nature of the active sites is still uncertain, despite the extensive research frequently undertaken on supported metallic (16–20) and oxidic (21–23) copper catalysts. Thus, from the study of the interaction of CO with oxygen adsorbed on Cu(100), (110), and (111) single-crystal by Habraken *et al.* it was concluded that the CO oxidation reaction proceeded via a Langmuir–Hinshelwood (LH) mechanism involving adsorbed CO molecules and oxygen atoms (16, 17). Choi and Vannice also arrive at the conclusion that the CO oxidation over supported, prereduced Cu crystallites proceeded through an LH mechanism invoking noncompetitive adsorption between $O_2$ and CO (20). They proposed that under reaction conditions the catalyst surface is a thin overlayer (two or three monolayers) of $Cu_2O$ with $O_2$ vacancies, allowing CO adsorption on exposed $Cu^+$ species, or possibly on $Cu_2O$/Cu interface sites, while $O_2$ would interact with Cu atoms to maintain the $Cu_2O$ layer. On the other hand, Boon *et al.* have demonstrated the importance of the oxygen vacancies in copper oxide for the oxidation of CO (21). Recently, Panayotov and Mehandjiev (22), in the study of the interaction of NO and CO, and mixtures of $O_2 + CO$, $NO + CO$, and $NO + O_2 + CO$, with the CuO surface, considered that under the reaction conditions $Cu^+$ and $Cu^0$ centers were formed. Consistent with this, in our previous studies of CO oxidation over alumina-supported copper oxide catalysts it was also found that $Cu^+$ and/or $Cu^0$ are the active sites for CO oxidation (15, 23). More recently, Jernigan and Somorjai (24) showed that the rate of CO oxidation at 573 K decreased with increasing copper oxidation state.

A problem inherent to these catalysts, mainly on the alumina-supported systems prepared by impregnation of alumina with metal salt solutions, is the possible presence of several phases or surface species of the metal. Thus, the oxidic $Cu/Al_2O_3$ catalysts generally contain CuO, a

[1] Deceased.
[2] Corresponding author. E-mail: alagudo@icp.csic.es.



0021-9517/98 $25.00

"surface Cu–$Al_2O_3$-like spinel" and bulk $CuAl_2O_4$, in concentrations which depend on the preparation conditions (11). The Cu–Cr/$Al_2O_3$ catalysts show an even more complicated picture. In addition to the above compounds, they can also contain $CuCr_2O_4$, $Cr_2O_3$, $Cr_3O_4$, and other possible compounds (25, 26).

Therefore, the variety of phases that may be present in these catalysts makes the interpretation of the catalytic results difficult. For example, in alumina-supported copper catalysts, an inverse relationship between catalytic activity and copper dispersion measured by XPS has been observed: the catalysts with low copper concentration showed a certain deactivation through use, whereas copper dispersion increased (15). The contrary was observed for chromium-containing catalysts (27). The copper chromite catalyst is another example in which an increase in catalytic activity upon pretreatment with carbon monoxide was of the same order of magnitude as the surface copper enrichment observed by AES (14). However, the origin of this surface copper enrichment has not been clarified.

Within the above scope, the objective of the present work is to study a simplified catalytic system by eliminating the support, in order to gain further insight into the nature of the copper species present on the surface of bulk $CuAl_2O_4$ and $CuCr_2O_4$ catalysts, to follow their transformation upon pretreatment and reaction, and to attempt to relate them with the catalytic behaviour for CO oxidation.

## EXPERIMENTAL

### *Catalyst Preparation*

The $CuAl_2O_4$ and $CuCr_2O_4$ catalysts were prepared by mixing the stoichiometric amounts of the corresponding nitrate salt solutions, followed by calcination as described previously (28). Briefly, the mixtures were evaporated slowly at 343 K with continuous stirring, dried at 383 K overnight, and calcined at 1223 K for 24 h. The mixed oxide $CuAl_2O_4$ and $CuCr_2O_4$ catalysts will be designated as CuAl and CuCr, respectively. The surface areas were 3 and $<1$ $m^2/g$, respectively. In order to remove single oxide impurities, such as CuO and/or $Cr_2O_3$, two extraction treatments were employed:

(i) An aliquot of the samples was treated with a 1 *M* $(NH_4)_2CO_3$ solution and maintained under vigorous stirring as reported elsewhere (29). Metal compound leaching is confirmed by the colour of the solutions which turned blue after treatment of $CuAl_2O_4$, and green in the case of $CuCr_2O_4$. Afterwards, the solids were separated by filtration and the procedure was repeated until no coloured solutions were observed. Finally, the samples were washed with distilled water until pH = 7 and dried at 383 K. The filtrates were collected and analysed by atomic absorption spectrometry.

(ii) Another aliquot was treated with a concentrated $HNO_3$ solution, following a procedure similar to that for the alkaline treatment. In this case, coloured solutions were observed only after induction periods, which means that the extent of metal leaching increases with its concentration in solution. The surface area of these leached samples were essentially unchanged. The leached catalyst samples will be designated as CuAl and CuCr, followed by a hyphen and AC or H for the treatments with ammonium carbonate or nitric acid, respectively.

### *Catalyst Characterization*

X-ray diffraction patterns were recorded with a Philips diffractometer PW 1730 with Cu anode and Ni filter. Approximate concentrations of the compounds were estimated from the intensity of the more intense XRD peak of each compound.

Temperature programmed reduction (TPR) experiments were carried out in a continuous flow system provided with a thermal conductivity detector. Details of the experimental setup can be found elsewhere (30). Catalyst reductions were performed either with mixtures of 15 vol% $H_2/N_2$ or 15 vol% CO/He. The heating rate was 20 K/min, and the total flow of the reduction mixture (reduction agent + diluent) was 30 ml/min. The characteristic peak temperatures, Tm, correspond to the maximum rate of $H_2$ consumption.

Photoelectron spectra were recorded with a Fisons ESCALAB 200R spectrometer equipped with a Mg K$\alpha$ X-ray source ($h\nu = 1253.6$ eV) and a hemispherical electron analyser. The X-ray source was operated at 120 W. The samples were ground to a fine powder and then pressed into small stainless steel cylinders and mounted onto a manipulator which allowed the transfer from the preparation chamber into the spectrometer. Before the analysis, they were outgassed or reduced in $H_2$ or CO atmospheres at 523 K. The residual pressure in the ion-pumped analysis chamber was maintained below $3 \cdot 10^{-9}$ Torr (1 Torr = 133.33 N · $m^{-2}$) during data acquisition. The C 1s peak at a binding energy of 284.9 eV was taken as an internal standard. The accuracy of BEs values was within ±0.2 eV. Ratios of the atomic concentrations in the outer surface layer of the catalysts were estimated from the corresponding XPS peak area ratios using the relation $Cu/M = (I_{Cu}/I_M)(\sigma_M/\sigma_{Cu})(\lambda_M/\lambda_{Cu})f(kE)$, where I, $\sigma$, and $\lambda$ are the normalized intensities (after s-shaped background substration), the effective ionization cross section, and the escape depth, respectively. The function $f(kE) = (kE_{Cu}/kE_M)^{0.5}$ (M = Al, Cr) was taken to account for the efficiency of the detector. Cross section determined by Scofield (31) and escape depths calculated by Penn (32) were used. The spectra were decomposed with the least squares fitting routine provided by the manufacturer with a Gaussian-to-Lorentzian ratio of 80/20 and after subtraction of an S-shaped (Shirley) background.

*Activity Measurements*

The catalytic activity for oxidation of CO was measured in a flow reactor at atmospheric pressure. Details of the apparatus and operation conditions have been described elsewhere (13, 28). The oxide catalyst samples were pretreated *in situ* at 573 K for 3 h in either CO or $H_2$. The temperature of reaction was maintained at 473 K. A mixture of 17% CO in air was employed as reactant feed, and the total flow was 180 ml $min^{-1}$. The catalyst samples (ranging from 0.05 to 0.40 g) were diluted to 2.5 g with alumina in order to obtain a catalytic bed of appropriate size.

## RESULTS

*X-Ray Diffraction and Extraction*

XRD patterns of the CuAl and CuCr catalysts (Figs. 1a and 1d) showed the typical diffraction lines of bulk $CuAl_2O_4$ and $CuCr_2O_4$, accompanied by small peaks of crystalline CuO in the CuAl sample, and both $Cr_2O_3$ and $Cr_3O_4$ in the CuCr catalyst. The extent of metal leached in basic and acid media from both CuAl and CuCr catalysts is presented in Table 1. By treatment with $(NH_4)_2CO_3$ only a small fraction of copper (0.15% as CuO) was removed in the CuAl catalyst. The XRD pattern of this leached sample (Fig. 1b) does not differ substantially from that of the original catalyst (Fig. 1a). Furthermore, aluminium was not detected in the extraction solution, confirming that the $CuAl_2O_4$ phase was not affected by the alkaline treatment. A similar amount of CuO (0.11%) and traces of $Cr_2O_3$ (~0.01%) were leached by $(NH_4)_2CO_3$ treatment from the CuCr sample (Table 1). However, copper oxide was not observed in the XRD pattern of the original CuCr sample (Fig. 1d), which remained essentially the same after $(NH_4)_2CO_3$ treatment (Fig. 1e). These results suggest that the copper extracted from both preparations was present as a very dispersed copper oxide phase not detectable by XRD. The treatment with ammonium carbonate solution seems to solubilize exclusively this copper oxide phase, leaving intact bulk crystalline copper oxide.

**TABLE 1**

**Catalyst Characterization by XRD and Metal Extraction**

| Catalyst | Phases detected by XRD[a] | Percentage metal extracted with $(NH_4)_2CO_3$ Cu[b] | $(NH_4)_2CO_3$ Cr[c] | $(NH_4)_2CO_3$ Al | $NHO_3$ Cu[b] | $NHO_3$ Cr[c] | $NHO_3$ Al |
|---|---|---|---|---|---|---|---|
| CuAl | $CuAl_2O_4$(94.7), CuO | 0.15 | — | n.d.[d] | 5.1 | — | n.d. |
| CuCr | $CuCr_2O_4$(84.8), $Cr_2O_3$, $Cr_3O_4$ | 0.11 | 0.01 | — | 0.12 | 0.03 | — |

[a] In parenthesis the percentage of the more abundant phase.
[b] Expressed as CuO.
[c] Expressed as $Cr_2O_3$.
[d] Not detected.

With the more severe $HNO_3$ treatment, the percentage of CuO removed from the CuAl sample was almost identical to the quantity of CuO estimated from XRD (Table 1). Also, as in the alkaline treatment, no aluminium was eliminated by the $HNO_3$ treatment. For the CuCr catalysts the results of extraction with $HNO_3$ were similar to those obtained with carbonate treatment; i.e., no additional elimination of simple oxides was observed (Table 1). Accordingly, no peaks of CuO appeared in the XRD pattern of the CuAl-H sample (Fig. 1c), while no significative changes were observed in the CuCr-H sample as compared to its untreated CuCr homologue (Figs. 1d and 1f).

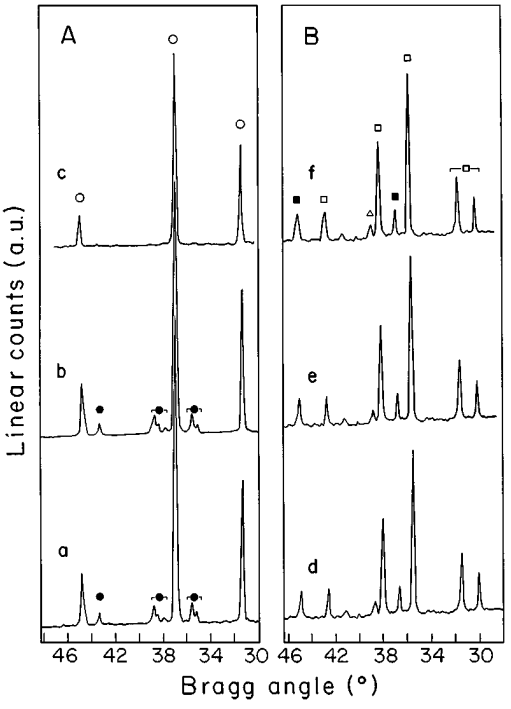


**FIG. 1.** XRD patterns of CuAl and CuCr catalysts: (a) CuAl; (b) CuAl-AC; (c) CuAl-H; (d) CuCr; (e) CuCr-AC; (f) CuCr-H; ○, $CuAl_2O_4$; ●, CuO; □, $CuCr_2O_4$; ■, $Cr_2O_3$; △, $Cr_3O_4$.

*X-Ray Photoelectron Spectroscopy*

The XPS binding energies (BE) of some characteristic core levels of Cu, Cr, Al, and O in CuAl and CuCr samples are compiled in Table 2. Regardless of the composition of the samples and of the extraction treatment employed, the wide Cu $2p_{3/2}$ signals obtained with all samples could be fitted satisfactorily to two principal peak components at about 935.3 and 933.8 eV for all the oxidic samples (Tables 2–4). The value of BE for the Cu $2p_{3/2}$ peak at 933.8 eV in CuAl is comparable with those reported for $Cu^{2+}$ in CuO (10, 12, 33, 34), while that at 935.3 eV is similar to the value given for $Cu^{2+}$ in $CuAl_2O_4$ (12, 35). Note, however, that the ratio of

**TABLE 2**

**Binding Energy Values (in eV) of CuAl and CuCr Catalysts**

| Catalyst | Cu $2p_{3/2}$ | Al 2p | Cr 2p | O 1s |
|---|---|---|---|---|
| CuAl | 933.9 | 74.5 | — | 531.9 |
| | 935.3 | | | 529.7 |
| CuAl-H | 933.8 | 74.5 | — | 530.7 |
| | 935.3 | | | |
| CuCr | 933.8 | — | 576.6 | 531.2 |
| | 935.2 | | | 529.4 |
| CuCr-H | 933.9 | — | 576.5 | 531.3 |
| | 935.3 | | | 529.6 |

intensities of the two peaks do not change upon treatment with $HNO_3$, although bulk CuO was removed with such treatment, as shown by XRD. Thus, an alternative assignation of the peaks to $Cu^{2+}$ coordinated tetrahedrally—high BE—and octahedrally—low BE—could be considered (see below).

The BE for the Al 2p peak was in close agreement with that for $Al^{3+}$ in $Al_2O_4^{2-}$-type compounds (10, 36), confirming that the main phase present is $CuAl_2O_4$. Some insight into the surface copper species can be derived from the analysis of the O 1s peak. The O 1s signal of the calcined sample shows two overlapping peaks at 531.9 and 529.7 eV (Fig. 2), assigned to lattice oxygen ions in different chemical environments. After $HNO_3$ treatment, Cu and Al signals remained the same as for the nonextracted samples, while the O 1s signal showed a single peak at 530.7 eV. As no aluminum was extracted by $HNO_3$, this suggests that the removed O 1s peak could be related to a copper oxidic species, probably CuO, in agreement with the XRD results and chemical analyses of extraction solutions.

The CuCr sample showed typical peaks of $Cu^{2+}$ (BE at 933.8 and 935.2 eV) and $Cr^{3+}$ (BE at 576.6 eV) and two peaks of $O^{2-}$ (BE at 529.4 and 531.2 eV) (Table 2). After leaching only a change in relative intensity of the O 1s peaks was observed (Fig. 2). In the case of copper chromites, similar Cu $2p_{3/2}$ signals have been reported elsewhere (37) and assigned to $Cu^{2+}$ located in two different types of sites. In general, the high BE signal is assigned to tetrahedrally coordinated sites (A-type sites of the spinel structure) while those at about 933.8 eV are assigned to spinel B-type sites, of octahedral symmetry (37, 38). Note that the same assignations could be made to the two signals observed in the case of the CuAl samples, although in that case the low BE signal must account for octahedral spinel sites of both $CuAl_2O_4$ and CuO.

The Cu $2p_{3/2}$ core level spectra of the three CuAl, CuAl-AC, and CuAl-H catalyst samples, outgassed and reduced with CO or $H_2$ are displayed in Fig. 3. The binding energies, reduction percentages, modified Auger parameter, and relative exposure of copper are compiled in Table 3. The fresh (unreduced) samples (Fig. 3A) showed two peaks at 933.8–933.9 and 935.2–935.3 eV, accompanied by the characteristic $Cu^{2+}$ shake-up satellite peak (33, 34). The intensity of the low BE peak is slightly higher than that of the high BE one, and washings do not change the relative sizes of the peaks. For these three fresh CuAl samples, no reduced copper was detected. The ratio of $Cu^{2+}$ satellite-to-principal Cu $2p_{3/2}$ peak ($I_{SAT}/I_{PP}$), between 0.67 and 0.72, was rather low as compared to the 1.1 values reported by Hercules *et al.* for $CuAl_2O_4$ (12). However, d'Huysser *et al.* have discussed that a normal spinel should present high $I_{SAT}/I_{PP}$ values, e.g., 0.86 for $CuCr_2O_4$ (36), while inverse spinels, such as $CuAl_2O_4$, must show lower values (37, 38). The modified Auger parameter ($\alpha A'$) of copper was used to unambiguously determine the chemical state of copper. This parameter is defined by

$$\alpha A' = 1253.6 + (\text{KE Cu}_{\text{LMM}} - \text{KE Cu } 2p_{3/2}), \qquad [1]$$

where KE $Cu_{LMM}$ and KE Cu $2p_{3/2}$ are the kinetic energies of the Auger electron and core-level photoelectron, respectively, and 1253.6 eV is the energy of the incident photons. The $\alpha A'$ values at 1851.2–1851.4 eV for the fresh CuAl samples allow us to conclusively establish that copper is present as $Cu^{2+}$ ions (4).

After reduction by CO (Fig. 3B and Table 3) the Cu 2p signal was transformed in three overlapping peaks at about 935.3, 933.7–933.8, and 932.8 eV. This fitting to three components was based on the fact that the position of the signals

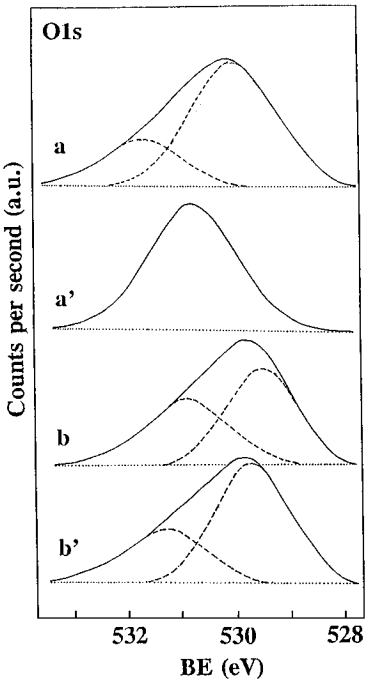


**FIG. 2.** O 1s core level spectra for CuAl and CuCr catalysts unleached and leached with $HNO_3$: (a) CuAl; (a′) CuAl-H; (b) CuCr; (b′) CuCr-H.

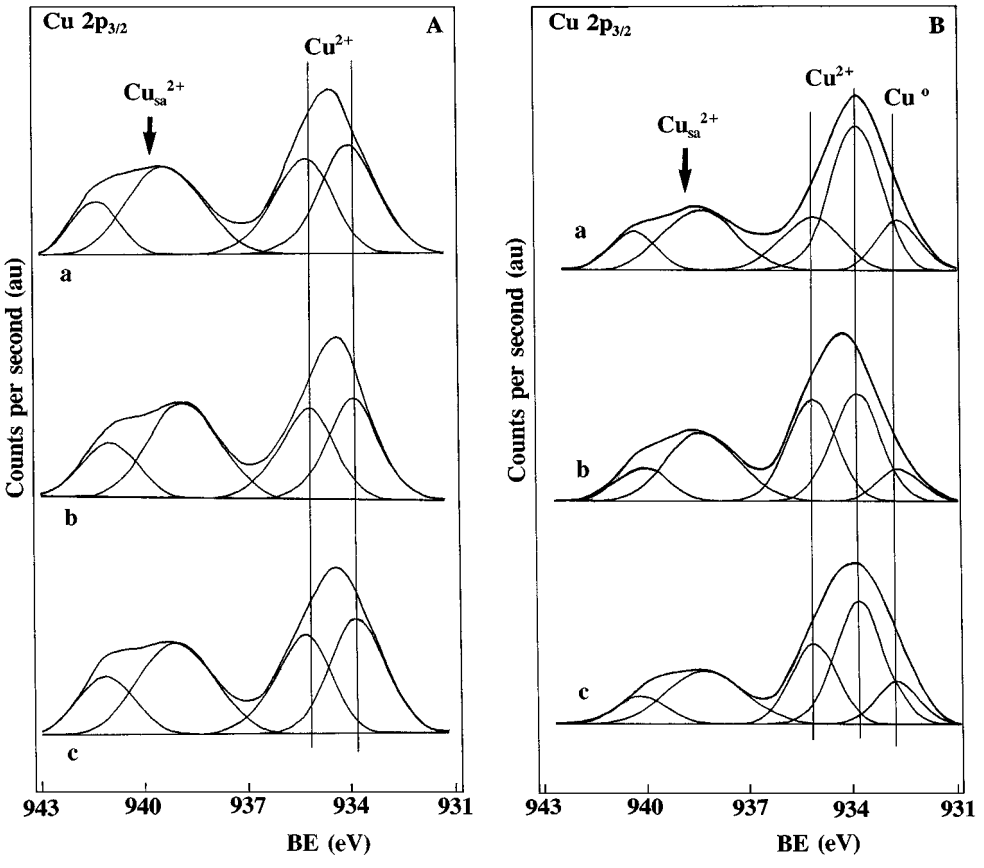


**FIG. 3.** Cu $2p_{3/2}$ core level spectra for CuAl catalysts: (A), unreduced samples; (B), CO reduced samples; (C), $H_2$-reduced samples. (a) CuAl; (b) CuAl-AC; (c) CuAl-H.

was different and the full width at half maximum (FWHM) was ca 1 eV wider than that for the parent outgassed samples. The first peak closely corresponds to the original peak assigned to $Cu^{2+}$[Th] in $CuAl_2O_4$. The second peak, at 933.7–933.8 eV, can be attributed, in agreement with the assignment of a similar peak of fresh outgassed samples, to $Cu^{2+}$[Oh] sites. Thus an important amount of copper remains unreduced, in agreement with the resistance of the spinel structure to reductive decomposition (39). The third peak at 932.8 eV fits well with metallic $Cu^0$, but it cannot be excluded that a small proportion of $Cu^+$ species could be also present. Comparison with the unreduced samples shows that the $Cu^{2+}$[Th] sites are reduced to a higher extent than the (Oh) ones, particularly for the CuAl sample. This finding agrees well with others in the study of reduction behaviour of $CuO/Al_2O_3$ catalysts (43). The fraction of reduced copper in these three CO-prereduced samples reaches values of 11–14% and simultaneously the ratio of satellite-to-principal peak decreases. It can also be noted that the CuAl-AC sample displays a somewhat lower percentage of reduced copper. For these samples, the $Cu_{LMM}$ peaks were broad, suggesting that more than one reduced copper species are formed. By applying peak synthesis procedures, two different values of the modified Auger parameter at 1851.2–1851.5 and 1849.3–1849.5 eV were observed. Whereas only $Cu^+$ species are responsible of the latter component, it is thought that both $Cu^{2+}$ and $Cu^0$ species may be involved in the former one.

When the reduction was carried out in $H_2$ (Fig. 3C) two peaks were observed: A very small peak at about 934.4–934.3 eV of $Cu^{2+}$, its satellite signal hardly being observable, and another more intense at about 932.7–932.9 eV, assigned to $Cu^0$. This assignment is supported by the small FWHM of the latter peak, which is characteristic of an ordered structure such as a Cu crystal, and also for the decrease of the ratio between the satellite line of copper and its principal Cu $2p_{3/2}$ peak ($I_{SAT}/I_{PP}$), summarized in Table 3. For these $H_2$-prereduced samples, the high percentages (87–90%) of metallic copper are accompanied by a strong decrease of satellite line ($I_{SAT}/I_{PP} = 0.15$–$0.23$). The Auger parameter ($1851.0 \pm 0.1$ eV) confirms that $Cu^0$ is the major copper species present at the surfaces of these samples.

For CuCr samples (Fig. 4 and Table 4), the Cu $2p_{3/2}$ signal of the outgassed CuCr, CuCr-AC, and CuCr-H unreduced

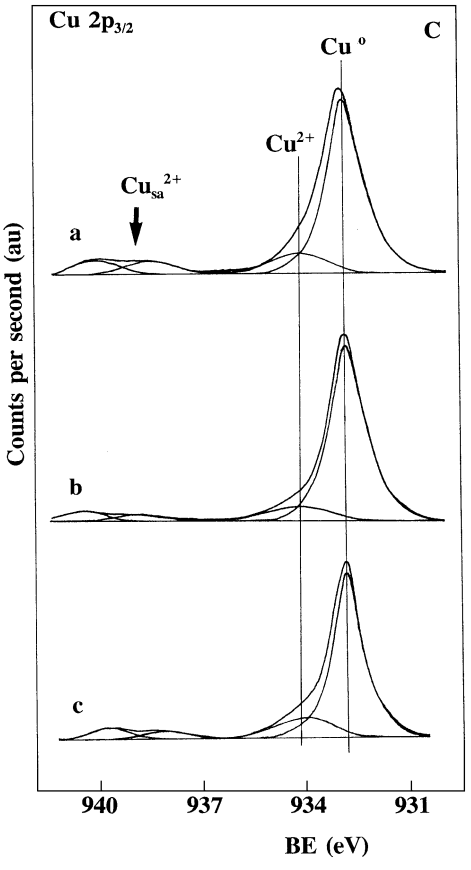


**FIG. 3**—*Continued*

samples showed two overlapping peaks (Fig. 4A): one at about 935.2 eV assigned to $Cu^{2+}$[Th], and another peak at about 933.8 eV attributed to $Cu^{2+}$[Oh]. In this case, the first (high BE) signal is larger than that due to octahedral sites. After washings, the difference is still more noticeable, suggesting preferential removal of octahedrally coordinated $Cu^{2+}$. The Auger parameter at ca 1851.2 eV is good evidence for copper in a $Cu^{2+}$ state (25, 40, 41). The Cr $2p_{3/2}$ core level spectrum of the CuCr samples (not shown) appeared at a BE near 576.5 eV, which is typical of $Cr^{3+}$ ions (14, 23). These Cr signals were practically unchanged irrespective of the washing procedures and reduction pretreatments.

Significant changes in the Cu $2p_{3/2}$ line profile were observed for the three CO-reduced CuCr samples (Fig. 4B). For these samples the Cu $2p_{3/2}$ line could be fitted to three components positioned at similar BE as for the CuAl counterparts. The first two have shapes and BEs similar to those of the unreduced samples, although it is clear than the peak at about 935.2 eV decreases strongly with respect to that at ~933.8 eV. The percentages of reduced copper ($Cu^0$) ranged between 22 and 32% and simultaneously the ratio of the satellite-to-principal peak decreased with respect to the unreduced samples. For the $H_2$-reduced CuCr samples (Fig. 4C), Cu $2p_{3/2}$ peaks were fitted to two components: a minor component at 934.3–934.4 eV associated to unreduced $Cu^{2+}$ ions in $CuCr_2O_4$ and a major one at 932.7–932.9 eV due to $Cu^0$. Metallic copper percentages for $H_2$-reduced CuCr samples were almost twice those of the CO-reduced counterparts while the $I_{SAT}/I_{PP}$ ratio decreased substantially. Although the $Cu_{LMM}$ line was rather broad, the measured $\alpha A'$ value indicated that the major copper species is $Cu^0$.

The relative exposure of copper at CuAl and CuCr catalyst surfaces has been evaluated by means of the equation: $Cu_{ex} = Cu/M$ (M = Al, Cr), where Cu/M is the atomic ratio of copper relative to aluminium or chromium. Quantitative results of total Cu and $Cu^0$ exposure are compiled in Tables 3 and 4. From these results, it is evident that the catalyst prereduction with CO and $H_2$ leads to a surface enrichment of the total copper exposure and the formation of metallic $Cu^0$, as compared to the outgassed samples. It is also clear that Cu exposure in CO-prereduced samples is about seven times higher on CuCr samples than on CuAl. Upon $H_2$-reduction, copper exposure for CuAl samples increased with respect to the CO-reduced samples, whereas Cu exposure drops strongly in CuCr with respect the CO-reduced counterparts. These tendencies suggest that, during reduction with CO, copper is segregated towards the CuAl and CuCr surfaces, where it suffers sintering whose extent is more important for CuAl samples. In other words, the copper phase generated under mild reduction conditions (CO) is more stable on CuCr samples than on CuAl.

*Temperature-Programmed Reduction*

As important differences in catalytic activity were observed when samples were pretreated with $H_2$ or CO (see below), the TPR spectra were recorded using the two reducing agents. The TPR of CuAl (Fig. 5) showed two main peaks with either $H_2$ or CO as reducing gas, the peak separation being larger in the case of reduction by CO. The first reduction peak at Tm between 528–549 K with CO and at 555–565 K with $H_2$, disappeared when the CuAl was treated with $HNO_3$ and bulk CuO was leached, according to the XRD results. The intensity of these low Tm peaks, however, corresponds to a larger extent of reduction than that due to the amount of CuO present (Table 5). Consequently, this low temperature peak is attributed only in part to crystalline CuO. It is possible that in the presence of bulk-like CuO part of the $Cu^{2+}$ ions from the spinel phase could be reduced while the single oxide is transformed to the metal. The high Tm bands are complex in shape, especially those found when reducing in CO. The difference in Tm between the higher temperature signals was large: in $H_2$ at 705 K; in CO at 1078 K. This shows that while CuO is easier to reduce in CO than in $H_2$, the reduction of $CuAl_2O_4$ is considerably more difficult in CO than in $H_2$. After alkaline treatment no significant differences with the fresh catalyst were detected.

**TABLE 3**

**XPS Analysis of $CuAl_2O_4$ Samples Subjected to Different Pretreatments**

| Pretreatment | Cu $2p_{3/2}$(eV) | $\alpha A'^{a}$ | %$Cu^0$ | Intensity ratio $Cu^{2+}_{sa}/Cu_{pral}$ | Atomic ratio Cu/Al | Atomic ratio $Cu^0$/Al |
|---|---|---|---|---|---|---|
| CuAl (vac) | 933.9<br>935.3 | 1851.4 | 0 | 0.69 | 0.48 | 0.0 |
| CuAl-AC (vac) | 933.8<br>935.2 | 1851.2 | 0 | 0.72 | 0.42 | 0.0 |
| CuAl-H (vac) | 933.8<br>935.3 | 1851.3 | 0 | 0.67 | 0.39 | 0.0 |
| CuAl (CO) | 932.8<br>933.8<br>935.2 | 1851.3<br>1849.3[b] | 14 | 0.56 | 1.55 | 0.22 |
| CuAl-AC (CO) | 932.8<br>933.8<br>935.1 | 1851.2<br>1849.5[b] | 11 | 0.64 | 1.34 | 0.15 |
| CuAl-H (CO) | 932.9<br>933.9<br>935.2 | 1851.5<br>1849.3[b] | 13 | 0.54 | 0.74 | 0.10 |
| CuAl ($H_2$) | 932.7<br>934.3 | 1850.9 | 87 | 0.23 | 1.72 | 1.49 |
| CuAl-AC ($H_2$) | 932.8<br>934.3 | 1851.0 | 90 | 0.15 | 2.00 | 1.80 |
| CuAl-H ($H_2$) | 932.9<br>934.4 | 1851.2 | 88 | 0.20 | 1.47 | 1.29 |

[a] The modified Auger parameter ($\alpha A'$) is defined by the equation: $\alpha A' = 1253.6 + (KE_{LMM} - KE\ Cu\ 2p_{3/2})$, where 1253.6 is the energy of the X-ray exciting source and $KE_{LMM}$ and KE Cu $2p_{3/2}$ are the kinetic energies of Auger copper line and photoemitted Cu $2p_{3/2}$ electron, respectively.

[b] Shoulder resolved by deconvolution.

The TPR profiles of the CuCr catalysts (Fig. 6) show broad signals with maxima in the 878–912 K region; the general shape of the peaks is slightly different in either reducing gas, showing asymmetry to the low Tm side in the case of $H_2$ and to the high Tm side with CO. In this sample, the $HNO_3$ treatment did not lead to peak disappearance, as observed for the CuAl-H sample. Only a small shoulder positioned at low Tm (about 788 K) was removed, which can be attributed to a very small amount of CuO. The asymmetry of the main signal could be the result of two closely overlapping peaks of similar intensities, reflecting reduction in two steps (from $Cu^{2+}$ to $Cu^+$ and then from $Cu^+$ to $Cu^0$).

*Catalytic Activity*

Catalytic activities, in the form of rate of CO conversion per gram ($r = ml\ min^{-1}\ g^{-1}$), of the catalysts at 473 K and after 5 h on-stream are shown in Fig. 7. It can be seen that the $(NH_4)_2CO_3$ treatment induced an increase in activity for both CuAl and CuCr catalysts. An additional increase resulted for the CuAl-H catalyst and practically no change occurred for the CuCr-H, as compared with its alkaline treated homologue. Pretreatment with $H_2$ produced higher activities for all the catalysts as compared to CO pretreatment. On the other hand, CuCr was generally more active than CuAl, whether the sample was unextracted or extracted, and irrespective of the reducing agent, except for the CO-reduced CuCr-Ac sample which had an activity comparable to that for the CO-reduced CuAl-Ac sample.

## DISCUSSION

As long as the formation of copper oxide is very common when mixed copper–metal oxides are prepared, different acid and alkaline extraction treatments have been developed to remove this impurity for characterization purposes (12, 29, 42). However, for catalytic studies it is necessary to take care in the nature of the extracting compound to avoid the incorporation of new impurities that can affect significantly the catalytic behaviour. For example, the HCl method (42) can affect the catalytic properties of the mixed oxide by incorporating the chloride ion. Thus, $(NH_4)_2CO_3$ extraction (29) appears to be the best among the methods reported, because this compound is very soluble and residual ammonium and carbonate should be removed by heating at low temperatures. However, in the present work, complete removal of CuO was not possible using the $(NH_4)_2CO_3$ treatment; only the fraction of amorphous or very dispersed CuO was removed. By applying

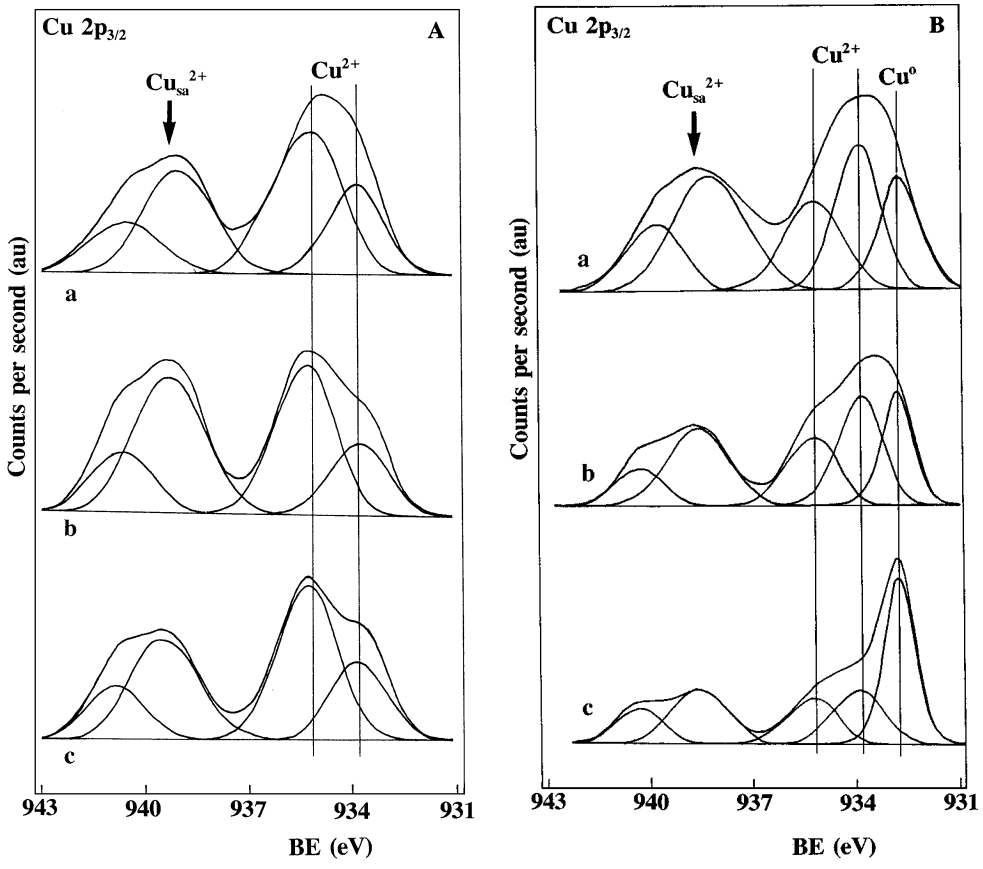


**FIG. 4.** Cu $2p_{3/2}$ core level spectra for CuCr catalysts: (A), unreduced samples; (B), CO reduced samples; (C), $H_2$-reduced samples. (a) CuCr; (b) CuCr-AC; (c) CuCr-H.

a stronger extraction with $HNO_3$ all unmixed copper oxidic species were apparently removed, including crystalline CuO, as shown by the bulk characterization techniques. Although the $Cr_2O_3$ and $Cr_3O_4$ impurities from the CuCr sample were not removed with either of the two treatments, these compounds were not active in the reaction conditions used in this work (27) and, therefore, no influence in the activity should be observed.

The results obtained in this study showed that untreated, and $(NH_4)_2CO_3$- and $HNO_3$-treated CuAl and CuCr samples provide interesting information about the different species present in the solids and their participation in the oxidation of CO. Thus, for CuAl the catalytic activity increased significantly after extraction with $(NH_4)_2CO_3$, particularly for the CO-pretreated sample, and even more for that extracted with $HNO_3$. This enhancement in activity is paralleled by a more or less complete removal of CuO, as revealed by XRD, chemical analysis, TPR, and XPS results. For CuCr, an increase in catalytic activity was also observed after $(NH_4)_2CO_3$ treatment, but no significant further increase occurs with $HNO_3$ extraction, which is consistent with no additional removal of CuO from the CuCr by this latter treatment. These changes in catalytic activity and the above characterization results indicate, in agreement with previous studies (10, 15, 20, 23), that the most important active centers for CO oxidation are associated to surface copper species in low oxidation states ($Cu^+$ and/or $Cu^0$) derived from the spinel-type structure. The CuO phase, present as an impurity on the catalyst surface, acts apparently as a diluent of the active sites due to its low activity and because the $Cu^0$ (from CuO) can be reoxidized directly to CuO, while $Cu^0$ (from a surface spinel) can be oxidized and stabilized as $Cu^+$. Hierl *et al.* (43) reported that the reoxidation of $H_2$-reduced $CuO/Al_2O_3$ samples with $O_2$ treatment at 953 K led to the formation in a first step of supported $Cu_2O$, which was then oxidized to supported CuO. The coexistence of $Cu^+$ on the catalyst surface seems to be essential for the catalytic activity (see below).

In fact, for both CuAl and CuCr samples maximum activity was found after prereduction, especially with $H_2$, conditions in which a high surface enrichment of total copper occurred, as compared to bulk concentration (14). Also, the presence of increasing amounts of reduced copper species in the surface was observed by XPS. Table 4

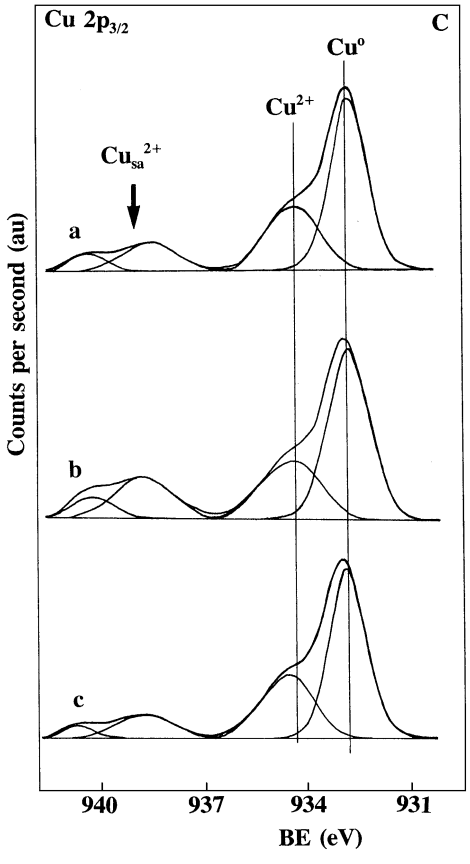


**FIG. 4**—*Continued*

shows that the surface of CO- and $H_2$-reduced CuCr catalysts appears highly enriched in metallic copper. These results are in agreement with our previous findings (14) and also with recent results of Makarova *et al.* (44), showing that migration of copper ions from the bulk $CuCr_2O_4$ spinel structure to the surface occurs by reduction in $H_2$. Hence, copper ions associated to the spinel-type structure are responsible for the observed Cu-enrichment on the surface of $CuCr_2O_4$ catalysts.

The higher activity of reduced copper has been recently demonstrated by Jernigan and Somorjai (24). These authors found the following order of activity: $Cu^0 > Cu^+ > Cu^{2+}$, when studying the oxidation of CO on a model catalyst system consisting of thin films of copper supported on graphite. The oxidation state of copper was controlled by proper choice of the reaction atmosphere and was monitored by XPS. Thus, not only the surface enrichment in total copper indicated above, but also an intrinsic enhancement of the activity is brought about by the reducing pretreatments since the catalyst surface is enriched in $Cu^0$. However, it must be noted that the activity difference between $Cu^0$ and $Cu^+$ decreased significantly when subsurface oxygen is present under the thin film of metallic copper (24). Also, Sadykov and Tikhov (45) in a recent comment pointed out that the results obtained on a thin layer catalyst model by Jernigan and Somorjai (24) cannot be extrapolated to bulk phases, where the defect structure of the solids influences the catalytic activity. In a similar way, it can be advanced that the changes in phase composition with the $O_2$/CO gas phase ratio observed in the case of thin layer or single-crystal catalytic models could not be valid for real catalysts. Thus, our previously obtained results showed substantial amounts of $Cu^+$ ions in reaction conditions characterized by experimental conditions similar to those employed in the present work by a high $O_2$/CO ratio, compared with that reported by Jernigan and Somorjai (24) for the range of stability of $Cu^+$ species.

Since the XPS results indicate that the reduced surface copper species consist predominantly, or only, of $Cu^0$ species, it can be thought, in principle, that such species may be the active sites for CO oxidation. Thus, a possible correlation between the rate of CO conversion to form $CO_2$ and the surface concentration of $Cu^0$ species was attempted. The $Cu^0$ concentration was calculated from the Cu/M (M = Al, Cr) atomic ratio and the percentage of reduced copper ($Cu^0$) obtained by XPS (Tables 3 and 4). No satisfactory linear correlation between activity per gram of catalyst and $Cu^0$ concentration was found and, particularly, for the CuCr samples in which the data appear highly scattered. Therefore, the surface concentration of $Cu^0$ species, as determined by XPS, does not seem to be the only factor determining the activity of these catalysts.

An alternative explanation to the observed phenomena could be the following. The prereduction of the catalysts within the XPS pretreatment chamber is likely more severe than that taking place under reaction conditions, in which the prereduced catalysts are brought in contact with the $CO + O_2$ mixture. Under reaction conditions, the formation of $Cu^+$ by reoxidation of some $Cu^0$ species is probable, since dispersed $Cu^0$ becomes easily oxidized. Consequently, it must lead to a coexistence of $Cu^0$ and $Cu^+$ species, as it seems to occur for the nonseverely CO-prereduced CuAl and CuCr samples according to XPS results. If the formation of $Cu^+$ species by CO-prereduction (or by instantaneous oxidation after admitting the CO + air feed) is appreciable, it should occur in a larger extent under reaction conditions. The present CuAl and CuCr catalysts were not examined by XPS under reaction conditions, but similar alumina-supported CuO and $CuCr_2O_4$ catalysts pretreated *in situ* in environments similar to that of reaction (i.e., pretreated in a CO + air mixture), were previously studied by XPS (23). The results showed that the dominant $Cu^0$ species present in CO-pretreated catalysts were transformed to a mixture of $Cu^0$ and $Cu^+$ species when they were exposed afterwards to a CO + air mixture similar to that used in the reaction and, also, that the observed catalyst deactivation caused by the addition of water was due to the oxidation of the $Cu^+$ and $Cu^0$ to $Cu^{2+}$ species. Other

**TABLE 4**

**XPS Analysis of $CuCr_2O_4$ Samples Subjected to Different Pretreatments**

| Pretreatment | Cu $2p_{3/2}$ (eV) | $\alpha A'$[a] | %$Cu^0$ | Intensity ratio $Cu^{2+}_{sa}/Cu_{pral}$ | Atomic ratio Cu/Cr | Atomic ratio $Cu^0$/Cr |
|---|---|---|---|---|---|---|
| CuCr (vac) | 933.8<br>935.2 | 1851.4 | 0 | 0.75 | 0.42 | 0.0 |
| CuCr-AC (vac) | 933.7<br>935.2 | 1851.2 | 0 | 0.85 | 0.37 | 0.0 |
| CuCr-H (vac) | 933.9<br>935.3 | 1851.2 | 0 | 0.79 | 0.35 | 0.0 |
| CuCr (CO) | 932.8<br>933.8<br>935.2 | 1851.2<br>1849.4[b] | 26 | 0.96 | 11.3 | 2.94 |
| CuCr-AC (CO) | 932.8<br>933.7<br>935.1 | 1851.2<br>1849.4[b] | 26 | 0.96 | 11.3 | 2.94 |
| CuCr-H (CO) | 932.9<br>933.9<br>935.2 | 1851.3<br>1849.2[b] | 32 | 0.67 | 7.0 | 2.24 |
| CuCr ($H_2$) | 932.7<br>934.3 | 1850.9 | 51 | 0.41 | 3.0 | 1.55 |
| CuCr-AC ($H_2$) | 932.8<br>934.3 | 1851.0 | 52 | 0.59 | 3.1 | 1.60 |
| CuCr-H ($H_2$) | 932.9<br>934.4 | 1851.1 | 50 | 0.43 | 3.0 | 1.50 |

[a] The modified Auger parameter ($\alpha A'$) is defined by the equation: $\alpha A' = 1253.6 + (KE_{LMM} - KE\ Cu\ 2p_{3/2})$, where 1253.6 is the energy of the X-ray exciting source and $KE_{LMM}$ and KE Cu $2p_{3/2}$ are the kinetic energies of Auger copper line and photoemitted Cu $2p_{3/2}$ electron, respectively.

[b] Shoulder resolved by deconvolution.

authors (20, 22, 46) have also proposed the coexistence of $Cu^0$ and $Cu^+$, or possibly $Cu_2O/Cu^0$ interface species, under steady-state reaction conditions over supported CuO catalyst. Choi and Vannice proposed a Langmuir–Hinshelwood

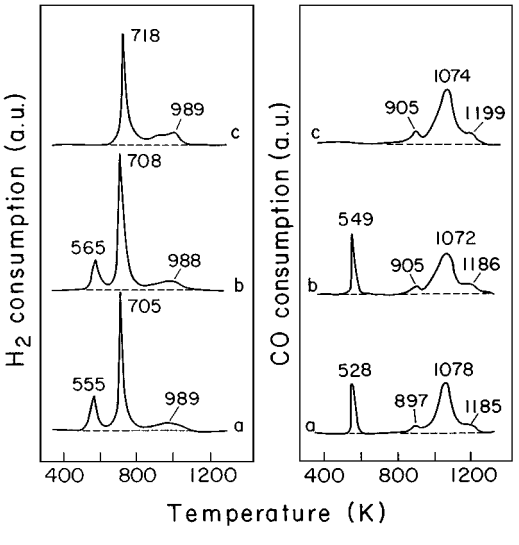


**FIG. 5.** TPR profiles of CuAl catalysts with CO and $H_2$: (a) CuAl; (b) CuAl-AC; (c) CuAl-H.

**TABLE 5**

**Quantitative Data Derived from TPR Profiles**

| Sample code | Weight (mg) | Cu content Ex-Cu[a] (mmole) | Cu content NEx-Cu[b] (mmole) | Amount of reducing gas Low Tm[c] (mmole) | Amount of reducing gas Total (mmole) |
|---|---|---|---|---|---|
| *Hydrogen* | | | | | |
| CuAl | 40.4 | 0.026 | 0.211 | 0.051 | 0.256 |
| CuAl-AC | 36.7 | 0.023 | 0.192 | 0.041 | 0.228 |
| CuAl-H | 41.7 | 0 | 0.230 | — | 0.242 |
| CuCr | 30.8 | — | 0.133 | — | 0.142 |
| CuCr-AC | 31.5 | — | 0.136 | — | 0.143 |
| CuCr-H | 29.0 | — | 0.125 | — | 0.128 |
| *Carbon Monoxide* | | | | | |
| CuAl | 39.7 | 0.025 | 0.208 | 0.053 | 0.260 |
| CuAl-AC | 43.9 | 0.028 | 0.230 | 0.055 | 0.285 |
| CuAl-H | 48.2 | 0 | 0.266 | — | 0.268 |
| CuCr | 34.6 | — | 0.149 | — | 0.140 |
| CuCr-AC | 37.0 | — | 0.160 | — | 0.166 |
| CuCr-H | 32.9 | — | 0.142 | — | 0.146 |

[a] Amount of Cu present as CuO (extractable by washings with $HNO_3$).

[b] Amount of Cu that cannot be extracted by treatment with $HNO_3$.

[c] Amount of reducing gas consumed in the peaks at 555–565 K ($H_2$) or 530–550 K (CO).

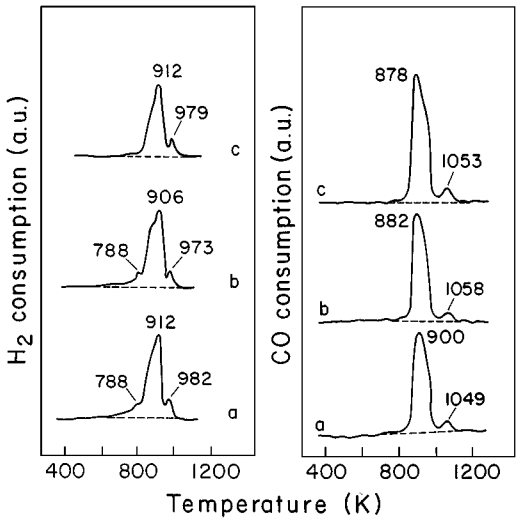


**FIG. 6.** TPR profiles of CuCr catalysts with CO and $H_2$: (a) CuCr; (b) CuCr-AC; (c) CuCr-H.

reaction mechanism between adsorbed CO molecules on surface $Cu^+$ species, or possibly on $Cu_2O/Cu^0$ interfaced sites, and chemisorbed O atoms on $Cu^0$ species (20). Furthermore, it was demonstrated that the reoxidation of $H_2$-reduced copper aluminate led to the formation in a first step of supported $Cu_2O$ (43). Thus, there seems to exist an extended agreement in the literature that both $Cu^0$ and $Cu^+$ are essential for CO oxidation on copper-based catalysts. The abundance and relative distribution of these two copper species on the catalyst surface during the reaction, which will depend essentially on the prereduction state of the catalyst and the gas phase composition during the reaction, will determine the catalytic activity. Once the copper is reduced to $Cu^0$ in the prereduction step, the reduced surface is partially oxidized during the course of the reaction and formation of $Cu^+$ to some extent would occur.

To check this hypothesis the Cu $2p_{3/2}$ core level and the X-ray induced Auger spectra of CuAl-H samples after reduction with $H_2$ and also subsequently treated under conditions similar to those of reaction (i.e., 300 Torr of 1/1 $CO/O_2$ ratio at 523 K for 1 h) in the preparation chamber of the spectrometer, were recorded. The XPS spectra of the Cu $2p_{3/2}$ peak of the reduced CuAl (Fig. 8A) and CuAl-H (Fig. 9A) catalysts were significantly changed

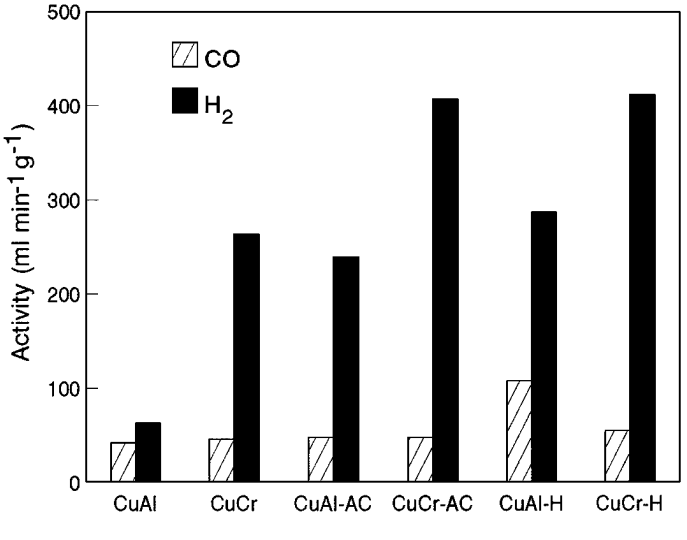


**FIG. 7.** Catalyst activity in CO oxidation at 473 K of the CuAl and CuCr catalysts.

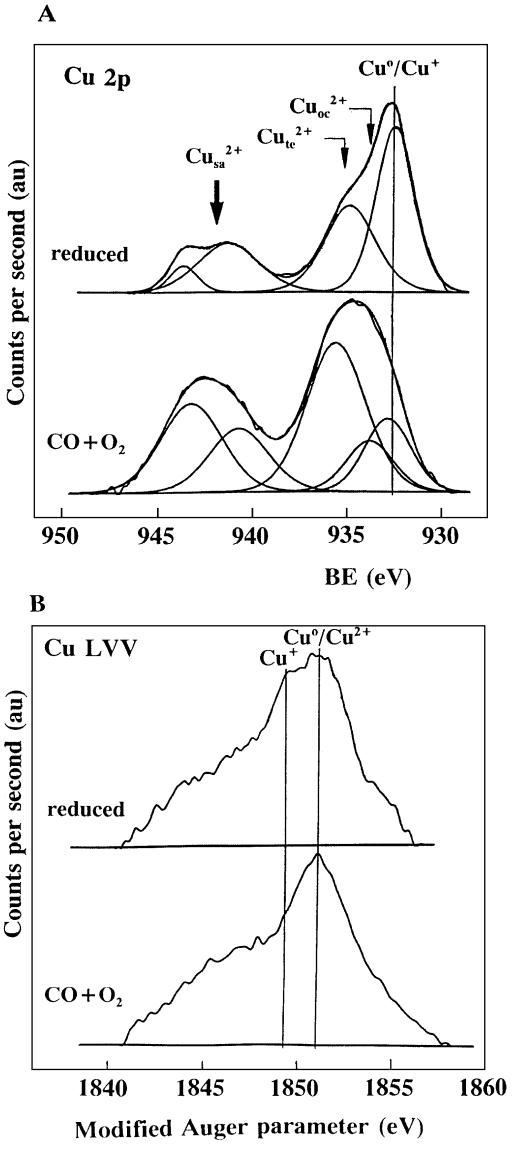


**FIG. 8.** Cu $2p_{3/2}$ core level spectra (A) and modified Auger parameter of copper for the CuAl catalyst subjected to reduction under $H_2$ at 523 K and subsequently exposed to the reaction mixture ($CO + O_2$) at 523 K for 1 h.

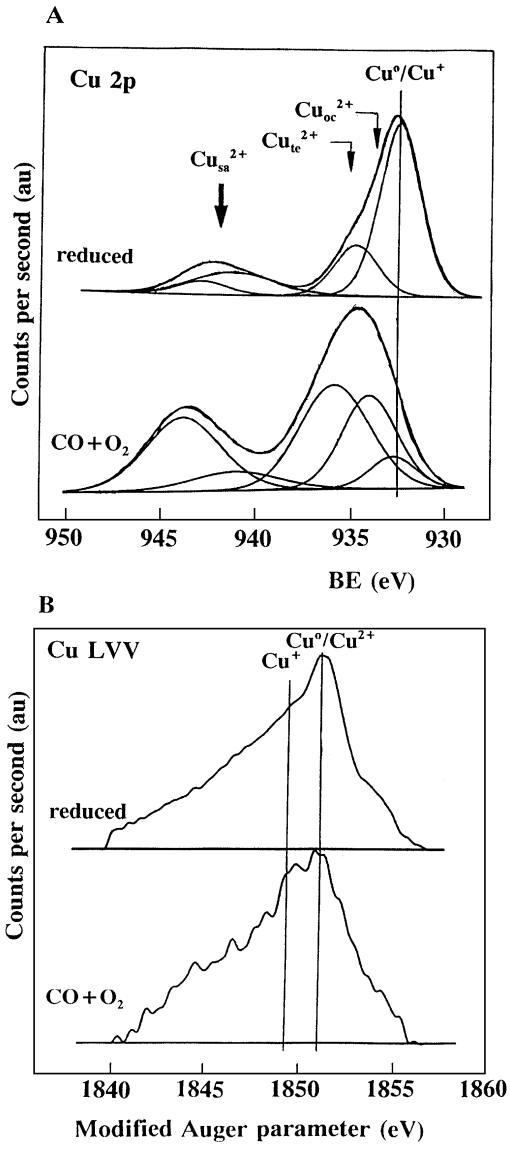


**FIG. 9.** Cu $2p_{3/2}$ core level spectra (A) and modified Auger parameter of copper for the CuAl-H catalyst subjected to reduction under $H_2$ at 523 K and subsequently exposed to the reaction mixture ($CO + O_2$) at 523 K for 1 h.

after exposure to the $CO + O_2$ reaction mixture, resulting in a broadening and a shift to higher BE of the Cu $2p_{3/2}$ signal, and the shake-up satellite peak increased significantly in intensity. Such changes in the XPS spectra are consistent with metallic copper being partially oxidized to $Cu^{2+}$ under reaction conditions for both CuAl and CuAl-H samples. The increased intensity of the Cu LVV peak around 1849 eV observed in the Auger parameter spectrum of the CuAl-H sample after being exposed to $CO + O_2$ (Fig. 9B) indicates the formation of $Cu^+$ species on the surface of this catalyst under reaction conditions, in agreement with our previous proposal. Obviously, these $Cu^+$ species result from the partial reoxidation of the metallic copper on the surface of the reduced $CuAl_2O_4$ spinel, since the amount of $Cu^0$ has significantly been reduced after $CO + O_2$ exposure, as the XPS spectrum shows (Fig. 9A). By contrast, in the surface of the CuAl catalyst after exposure to the $CO + O_2$ mixture (Fig. 8B) the $Cu^+$ species are not detected; apparently all the reoxidized metallic copper and, also, the initial $Cu^+$ species, formed during the prereduction step, have been completely oxidized to $Cu^{2+}$ and, therefore, this catalyst is less active than the CuAl-H one. The nonstabilization of $Cu^+$ species on the surface of the CuAl catalyst under the reaction conditions used is thought to be due to the presence of some bulk CuO on the surface catalyst and its mechanism of reduction and reoxidation. Thus, these results show the important role played by the $Cu^+$ species on the oxidation of CO over copper-based catalysts.

As the CuAl and CuCr catalysts have a spinel structure that is generally difficult to reduce, it is evident that prereduction with CO may lead to a catalyst surface relatively that is poorly reduced and, therefore, with low catalytic activity, while prereduction with $H_2$ should lead to a catalyst surface that is highly reduced and thus with higher activity. The TPR profiles of the CuAl samples confirmed the difference in reducibility with CO and $H_2$; the high Tm peak (due to the mixed oxides) is at a lower temperature with $H_2$ than with CO. In the case of the CuCr samples, the differences in the TPR profiles were rather in the extent of reduction and the relative proportion of the two high temperature overlapped peaks than in their position. However, these apparently small differences in reducibility seem to exert a large influence on the activity of the CuCr samples. The appearance of two overlapped peaks of similar sizes in the TPR of CuCr samples suggests a reduction in two steps: from $Cu^{2+}$ to $Cu^+$ (first peak) and from $Cu^+$ to $Cu^0$ (second peak). This is consistent with previous findings that the reduction of $CuCr_2O_4$ by $H_2$ at 493 K led initially to cuprous chromite $Cu_2Cr_2O_4$ (47). These steps are not observed in the CuAl samples because the direct reduction of $Cu^{2+}$ to $Cu^0$ is favoured. $CuCr_2O_4$ is a normal spinel without distortion (48, 49) and with 90% of $Cu^{2+}$ in tetrahedral sites in the surface (37), while $CuAl_2O_4$ is a cubic spinel with a tetragonal distortion (11) and only 60% of $Cu^{2+}$ in tetrahedral sites (11, 42). These structural differences probably result in different reduction mechanisms and also can account for the easier $H_2$-reduction of the CuAl samples, as compared with the CuCr samples, as shown by Figs. 5 and 6. This is consistent with the higher extent of reduced copper which was obtained by XPS for the $H_2$-reduced CuAl catalysts as compared to their CuCr counterparts (Tables 3 and 4). Despite the high reductions reached by the $H_2$-reduced CuAl samples, they had lower activities because the copper concentrations in the surface layers was approximately half that present on the CuCr samples reduced by $H_2$. Another important parameter which may also influence the catalytic

behaviour is the stability of the reduced $Cu^+$ species. Such a species can hardly be stabilized in a $CuAl_2O_4$ spinel structure for electroneutrality reasons (10), while on $CuCr_2O_4$ it seems to be stabilized through the formation of surface $Cu_2Cr_2O_4$, as result of the reduction of well-dispersed CuO on $CuCr_2O_4$ (49), or Cu occupying a defective $CuCr_2O_4$ structure (14). Thus the role of chromium seems to be to avoid the aggregation of the dispersed $Cu^0$, stabilizing a certain concentration of $Cu^+$ under reaction conditions.

It should be noted that, contrary to present work, alumina-supported copper catalysts calcined at 773 K were found to be more active when pretreated with CO instead of $H_2$ (15). A possible explanation for this contradiction is the formation by calcination at 773 K of species which are not stable upon firing at 1223 K. These species could be sites or local defects in the crystal lattice, with more coordination vacancies which may lead to different carbonyl species more active than those derived from the precursor calcined at 1223 K. The formation of copper carbonyl compounds in the catalysts calcined at 773 K was previously postulated (15, 27), suggesting a possible participation of carbonyl species in the redox mechanism involved in the catalytic oxidation of CO.

Finally, we want to point out, on the basis of the present results and previous findings (13–15, 27, 28), that the specific nature of the copper active sites seem to be greatly sensitive to the conditions of preparation and pretreatment and, also, to its coordination in the structure. Consequently, the activity of the Cu-based catalysts in CO oxidation will be strongly dependent on the mentioned parameters.

## CONCLUSIONS

The catalytic activity for CO oxidation of Cu and Cu–Cr oxide catalysts can be significantly increased by washing the catalyst powders with alkaline or acid solutions in order to remove low-activity precursor phases such as bulk CuO remaining on the catalyst surface. The nitric acid treatment has a stronger effect than ammonium carbonate treatment because of its large extraction of CuO. The extraction of less active bulk CuO enhances the formation of more active surface reduced copper species ($Cu^+$ and/or $Cu^0$) derived from the spinel-type structure in the prereduction state of the catalyst and under reaction conditions. The CuO phase acts apparently as a diluent of the active sites. Prereduction with $H_2$ leads to higher surface concentration of reduced copper species than prereduction with CO and thus higher activity. As such reduced copper species can be stabilized in a $CuCr_2O_4$ spinel more than in the parent $CuAl_2O_4$, the former sample presents higher activity than the latter one.

## ACKNOWLEDGMENT

Support for this work from the Scientific Cooperation Program with Iberoamerica, Ministerio de Educación y Ciencia of Spain, is gratefully acknowledged. Special thanks to Mrs. M. Labady, Mr. J. C. de Jesús, and Dr. A. Calafat for their collaboration.

## REFERENCES

1. Newsome, D. S., *Catal. Rev.-Sci. Eng.* **21**, 275 (1980).
2. Katz, M., *Adv. Catal.* **5**, 177 (1953).
3. Bart, J. C. J., and Sneeden, R. P. A., *Catal. Today* **2**, 1 (1987).
4. Fierro, J. L. G., "Properties and Applications of Perovskite-type Oxides" (L. G. Tejuca and J. L. G. Fierro. Eds.), p. 255. Marcel Dekker, New York, 1993.
5. Stone, F. S., *Adv. Catal.* **13**, 1 (1962).
6. Shelef, M., Otto, K., and Gandhi, H., *J. Catal.* **12**, 361 (1968).
7. Yu-Yao, Y. F., *J. Catal.* **39**, 104 (1975).
8. Kapteijn, F., Stegenga, S., Dekker, N. J. J., Bijsterbosch, J. W., and Moulijn, J. A., *Catal. Today* **16**, 273 (1993).
9. Stegenga, S., van Soest, R., Kapteijn, F., and Moulijn, J. A., *Appl. Catal. B: Environmental* **2**, 257 (1993).
10. Ertl, G., Hierl, R., Knözinger, H., Thiele, N., and Urbach, H. P., *Appl. Surf. Sci.* **5**, 49 (1980).
11. Friedman, R. B., Freeman, J. J., and Lytle, F. W., *J. Catal.* **55**, 10 (1978).
12. Strohmeier, B. R., Leyden, D. E., Scottfield, R., and Hercules, D. M., *J. Catal.* **94**, 514 (1985).
13. Severino, F., Brito, J., Carias, O., and Laine, J., *J. Catal.* **102**, 172 (1986).
14. Laine, J., Brito, J., Severino, F., Castro, G., Tacconi, P., Yunes, S., and Cruz, J., *Catal. Lett.* **5**, 45 (1990).
15. Laine, J., Severino, F., López Agudo, A., and Fierro, J. L. G., *J. Catal.* **129**, 297 (1991).
16. Habraken, F. H. P., and Bootsma, G. A., *Surf. Sci.* **87**, 333 (1979).
17. Habraken, F. H. P., Bootsma, G. A., Hofmann, P., Hachicha, S., and Bradshaw, A. M., *Surf. Sci.* **88**, 285 (1979).
18. van Pruissen, O. P., Dings, M. M. M., and Gizenau, O. L. J., *Surf. Sci.* **179**, 377 (1987).
19. Choi, K. I., and Vannice, M. A., *J. Catal.* **131**, 1, 36 (1991).
20. Choi, K. I., and Vannice, M. A., *J. Catal.* **131**, 22 (1991).
21. Boon, A. Q. M., van Looij, F., and Geus, J. W., *J. Mol. Catal.* **75**, 277 (1992).
22. Panayotov, D., and Mehandjiev, D., *Stud. Surf. Sci. Catal.* **75**, 1449 (1993).
23. López Agudo, A., Palacios, J. M., Fierro, J. L. G., Laine, J., and Severino, F., *Appl. Catal. A: General* **91**, 43 (1992).
24. Jernigan, G. G., and Somorjai, G. A., *J. Catal.* **147**, 567 (1994).
25. Poole, C. P., and Mac Iver, D. S., *Adv. Catal.* **17**, 223 (1967).
26. Jagannathan, K., Srinivasan, A., and Rao, C. N. R., *J. Catal.* **69**, 418 (1981).
27. Laine, J., Severino, F., López Agudo, A., and Fierro, J. L. G., *Stud. Surf. Sci. Catal.* **68**, 467 (1991).
28. Severino, F., and Laine, J., *Ind. Eng. Chem. Prod. Res. Dev.* **22**, 396 (1983).
29. Ketchik, S. V., Plyasova, L. M., Seredkin, A. E., Kostrov, V. V., and Morozov, L. N., *React. Kinet. Catal. Lett.* **14**, 429 (1980).
30. Brito, J., and Laine, J., *Polyhedron* **5**, 179 (1986).
31. Scofield, J. H., *J. Electron Spectr. Relat. Phenom.* **8**, 129 (1976).
32. Penn, D. R., *J. Electron Spectr. Relat. Phenom.* **9**, 29 (1976).
33. Fiermans, L., Hoogewiis, R., and Venik, J., *Surf. Sci.* **47**, 1 (1975).
34. Laine, J., Ceballos, G., Severino, F., Castro, G., and Rojas, C., *Catal. Lett.* **10**, 11 (1991).

35. Wolberg, A., Ogilvie, J. L., and Roth, J. F., *J. Catal.* **49**, 86 (1970).
36. Patterson, T. A., Carver, J. C., Leyden, D. E., and Hercules, D. M., *J. Phys. Chem*. **80**, 1702 (1976).
37. d'Huysser, A., Wrobel, G., and Bonnelle, J. P., *Nouv. J. Chim*. **6**, 437 (1982).
38. D'Huysser, A., Le Calonnec, D., Lenglet, M., Bonnelle, J. P., and Jørgensen, C. K., *Mater. Res. Bull.* **19**, 1157 (1984).
39. Plyasova, L. M., Solevyeva, L. P., Krieger, T. A., Makarova, O. V., and Yurieva, T. M., *J. Mol. Catal. A: Chemical* **105**, 61 (1996).
40. Fierro, J. L. G., *J. Phys. C: Cond. Matter* **5**, A229 (1993).
41. Sepúlveda, A., Márquez, C., Guerrero-Ruíz, A., Rodríguez-Ramos, I., and Fierro, J. L. G., *Surf. Interf. Anal.* **20**, 1067 (1993).
42. Marques, E. C., Friedman, R. M., and Dahm, D. J., *Appl. Catal.* **19**, 387 (1985).
43. Hierl, R., Knözinger, H., and Urbach, H. P., *J. Catal.* **69**, 475 (1981).
44. Makarova, O. V., Yurieva, T. M., Kustova, G. N., Ziborov, A. V., Plyasova, L. M., Minyokova, T. P., Davydova, L. P., and Zaikovskii, M., *Kinet. Catal.* **34**, 681 (1993).
45. Sadykova, V. A., and Tikhov, S. F., *J. Catal.* **165**, 279 (1997).
46. Sakurai, K., Okamoto, Y., Imanaka, T., and Teranishi, S., *Bull. Chem. Soc. Jpn*. **49**, 1732 (1976).
47. Tonner, S. P., Wainwright, M. S., Trimm, D. L., and Cant, N. W., *Appl. Catal.* **11**, 93 (1984).
48. Wells, A. F., "Structural Inorganic Chemistry," 3rd ed., pp. 457, 487. Oxford Univ. Press, London, 1962.
49. Wyckoff, R. W. G., "Crystal Structures," 2nd ed., Vol. 3, Interscience, New York, 1965.